Anna ANDRIJANOVITS[1], Andrei BLINOV[1], Dmitri VINNIKOV[1], João MARTINS[2]

Tallinn University of Technology (1), Universidade Nova de Lisboa-FCT-DEE and UNINOVA-CTS (2)

Magnetically Coupled Multiport Converter with Integrated Energy Storage

Abstract. *This paper presents a new integrated DC/DC converter for hydrogen-based energy storages. As compared to traditional individual converter based solutions for interfacing of an electrolyzer and a fuel cell, the proposed topology features reduced energy conversion stages. In order to improve the response time of the hydrogen buffer a battery was integrated into the interface converter with no need for an extra charging/discharging circuit. The paper analyzes and discusses the operating principle of the new converter and provides some design guidelines. Finally, theoretical background is experimentally verified.*

Streszczenie. *W artykule przedstawiono nową zintegrowaną przetwornicę DC / DC dla magazynów energii na bazie wodoru. W porównaniu do tradycyjnych rozwiązań z oddzielnymi przetwornicami do elektrolizera i ogniwa paliwowego, proponowaną topologię cechuje zmniejszona liczba etapy konwersji energii. W celu poprawienia czasu reakcji bufora wodorowego akumulator został zintegrowany z interfejsem przetwornicy, bez konieczności stosowania dodatkowego obwodu ładowania/rozładowania. W artykule przedstawiono analizę i omówiono zasady działania nowego przekształtnika, i podano wybrane zalecenia projektowe. W końcowej części przedstawiono wyniki eksperymentalne, weryfikujące założenia teoretyczne (**Wieloterminalowa przetwornica o sprzężeniu magnetycznym z zintegrowanym zasobnikiem energii)***

Keywords: electrolyzer, fuel cell, hydrogen buffer, multiport converter.
Słowa kluczowe: elektrolizer, ogniwo paliwowe, bufor wodoru, przekształtnik wieloportowy.

Introduction

In recent years, hydrogen-based long-term energy storages implemented in a renewable energy system (RES) have attracted much attention [1-4]. Essential elements of such a hydrogen buffer (HB) are an electrolyzer (EL), a hydrogen storage system and a fuel cell (FC). To achieve proper voltage matching the main components of the HB should be connected to the DC-bus of the RES via different power electronic converters: the EL is interfaced by help of a step-down DC/DC converter, while the FC is connected by help of a step-up DC/DC converter. Moreover, the battery should have a special charger circuit that integrates it to the DC-bus of a DES. It finally leads to complex multiconverter systems with a high number of energy conversion stages, complex control and reduced efficiency. The main trend in technology development here is to reduce the power losses in the interface converters to obtain the highest possible energy efficiency of the HB.

Recently a new integrated (multiport) DC/DC converter for HB interfacing in the RES was proposed [5]. Thanks to the implemented multiport converter concept (Fig. 1) the number of energy conversion stages was significantly reduced.

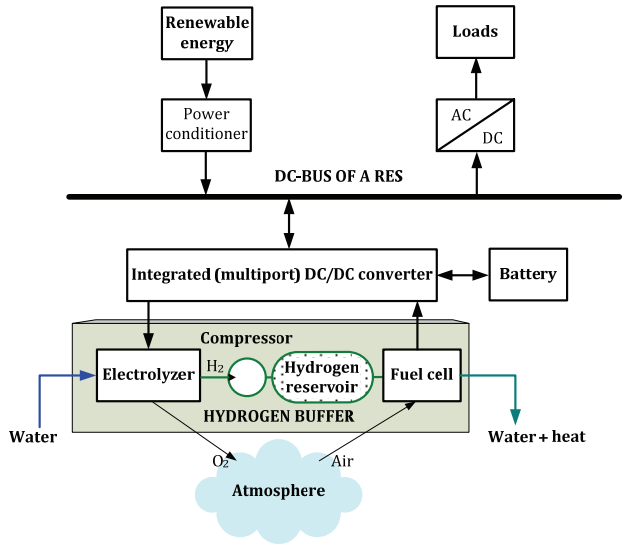

Fig. 1. Typical structure of the distributed energy system with the hydrogen buffer interfaced via multiport DC/DC converter

The resulting advantages of the proposed solution include reduced component count, lower cost, and control simplicity. Furthermore, the multiport converter technology may best satisfy integrated power conversion, efficient thermal management, compact packaging, and centralized control requirements [6, 7]. These advantages can potentially improve the overall cost, efficiency and flexibility of the hydrogen buffers used in the RES.

This paper discusses a possibility for further improvement of the hydrogen buffer with multiport DC/DC converter proposed in [5] by integrating the battery into the fuel cell side port. To decrease switching losses and improve the overall performance of the converter the half-bridge RES-side inverter was replaced with a three-level neutral point clamped (3L-NPC) voltage source inverter.

Basics of hydrogen buffers

Hydrogen is one of the promising alternatives that can be used as an energy carrier. The universality of hydrogen implies that it can replace other fuels for stationary generating units for power generation in various industries. Having all the advantages of fossil fuels, hydrogen is free of harmful emissions when used with dosed amount of oxygen, thus reducing the greenhouse effect [8].

Hydrogen based energy storage system or HB includes the following main stages: hydrogen production, hydrogen storage and electricity production [15]. In the excess energy periods the hydrogen generation system is connected to the DC-bus of the RES. In this stage electrical energy from the RES is converted into chemical energy by using water electrolysis and this energy is stored in a tank. In order to stabilize energy production during the absence of the renewable energy when more power is needed, stored hydrogen could be re-used. In this stage, hydrogen is converted into electrical energy by using a FC. The FC takes the hydrogen from the tanks to generate electricity, plus water and heat as by-products. Combination of an energy storage system and an RES allows controllable power production.

Water to hydrogen conversion efficiency is averaged at 65 % and FC conversion efficiency is 65-70 %, which yields an overall efficiency of the HB at 20-40% [9-11]. Since the FC has a slow response time and prefers to be operated under constant power, a battery is often used as an additional energy storage.

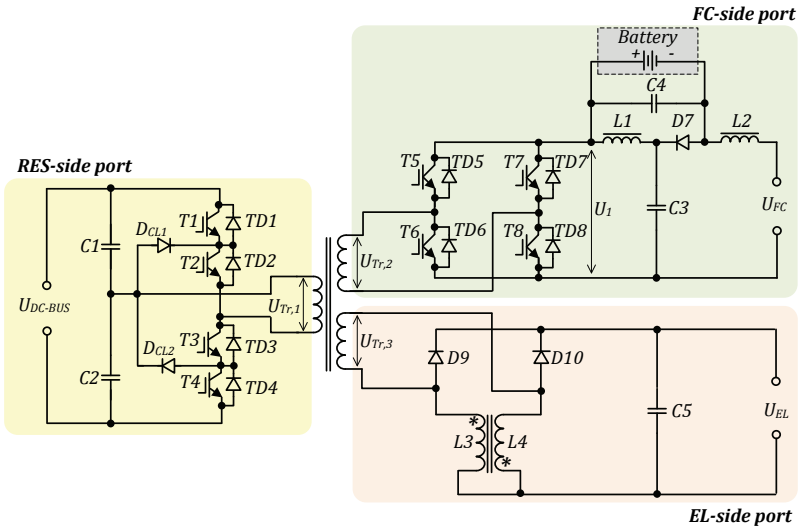

Fig. 2. Power circuit layout of the multiport converter with integrated energy storage

Generalized operation principle of the multiport converter with integrated energy storage

In the proposed multiport structure (Fig. 2) the EL and the FC are magnetically coupled with the RES-side converter by help of a multiwinding voltage matching transformer. Thus, all the ports of the converter are galvanically isolated, which could be a compulsory requirement for safety reasons in RES applications. The proposed converter consists of three ports: two unidirectional low-voltage ports for the interconnection of the EL and the FC and one high-voltage bidirectional port for the interconnection of the hydrogen buffer with the main DC-bus of a RES. There are two main operation modes of the integrated converter:

a) The EL operation mode. In this mode the surplus power from the DC-bus of a RES is supplying the electrolyzer and the multiport converter acts as a step-down converter.

b) The FC operation mode. In this mode electricity is generated by the fuel cell to cover the power deficiency in the DC-bus of the RES and the multiport converter acts as a step-up converter. In the FC operation mode several submodes could also be distinguished:

1) Battery assisted mode: the FC and the battery provide both the power to the DC-bus to manage the peak power demand.
2) Battery charging mode: FC power is higher than the load demanded power, the battery being charged from the FC.
3) Battery stand-by mode: the battery is fully charged and the fuel cell provides full power only to the DC-bus.
4)

A. EL operation mode

In the EL operation mode the converter acts as a traditional step-down isolated DC/DC converter with a 3L-NPC voltage-source inverter (VSI), a step-down isolation transformer and a current-doubler rectifier (Fig. 3). Implementation of a three-level half-bridge inverter with the PWM control algorithm presented in [12] allows all transistors of the inverter to be operated under the ZVS without additional components merely utilizing parasitic elements of the circuit, such as junction and freewheeling diode capacitances across each IGBT, and leakage inductance of the isolation transformer. In addition, the current doubler rectifier introduced with coupled inductors offers loss reduction in the secondary side of the converter in contrast to the traditional full-bridge rectifier due to the twice reduced operation current of the rectifier diodes and the secondary winding of the transformer.

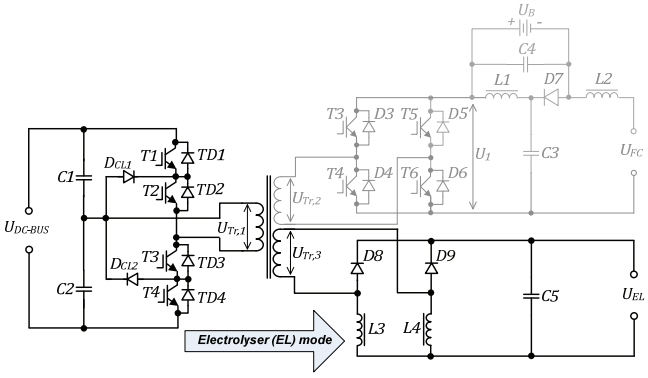

Fig.3. Power circuit configuration in the electrolyser (EL) mode

The EL voltage could be controlled by the duty cycle variation of the transistors *T1…T4*. Neglecting losses in the components, the voltage U_{EL} during the EL mode is

$$U_{EL} = \frac{U_{DC-BUS}}{2 \cdot n_1} \cdot D, \quad (1)$$

where U_{DC-BUS} is the DC-bus voltage of the main system (input voltage of the converter), D is the duty cycle of the inverter switches (*T1…T4*) and n_1 is the turns ratio of the isolation transformer windings 1 and 3:

$$n_1 = \frac{U_{Tr,1}}{U_{Tr,3}}, \quad (2)$$

where $U_{Tr,1}$ and $U_{Tr,3}$ are the amplitude voltages of the primary (high-voltage, DC-bus side) and tertiary (low-voltage, EL side) windings of the isolation transformer, respectively.

B. FC operation mode

In the FC operation mode the converter acts as a step-up isolated DC/DC converter and the power flows from the FC to the high-voltage DC-bus, thus performing the power back-up function. The configuration of the power circuit in FC mode is presented in Fig. 4.

The power flow from the FC to the DC-bus is controlled by the quasi-impedance-source inverter (qZSI). This inverter is operated with continuous input current [13], which is a very important property since FC systems are limited power sources and cannot handle rapid changes in the current they produce. The integrated freewheeling diodes *TD1…TD4* of transistor modules *T1…T4* together

with capacitors *C1* and *C2* act as the voltage-doubler rectifier. In the conditions of changing FC voltage the amplitude voltage $U_{Tr,2}$ of the secondary winding of the isolation transformer is kept constant by the variation of the duration of a shoot-through switching state of the qZSI. The shoot-through switching state is the simultaneous conduction of both switches of the same phase leg of the qZSI. This switching state is forbidden for the traditional voltage source converters because it could destroy the inverter. In the qZSI, the shoot-through states are used to store the magnetic energy in the DC-side inductors *L1* and *L2* without short-circuiting the DC-capacitors *C3* and *C4*. This magnetic energy in turn provides the boost of the voltage $U_{Tr,2}$ seen on the transformer secondary winding during the active states of the qZSI [14].

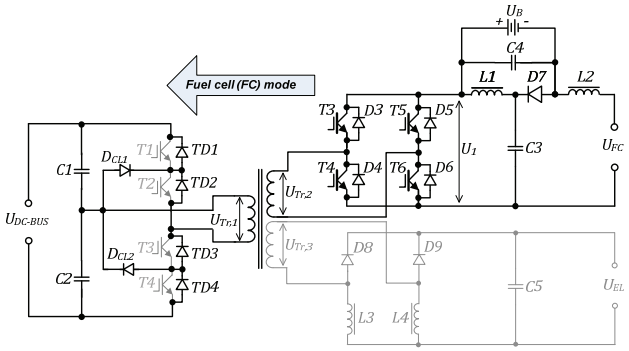

Fig.4. Power circuit configuration in the fuel cell (FC) mode

Neglecting losses in the components, the voltage U_{DC-BUS} during the FC mode could be regulated by the variation of a shoot-through duty cycle D_S:

(3) $$U_{DC-BUS} = \frac{2 \cdot U_{FC}}{n_2 \cdot (1 - 2 \cdot D_S)},$$

where U_{FC} is the fuel cell voltage, D_S is the shoot-through duty cycle of the qZSI switches (*T3*… *T6*). FC-side and RES-side ports of the converter are magnetically coupled through the isolation transformer's secondary and primary windings, respectively (Fig. 4) and the desired turns ratio of the isolation transformer n_2 is

(4) $$n_2 = \frac{U_{Tr,2}}{U_{Tr,1}},$$

where $U_{Tr,1}$ and $U_{Tr,2}$ are the amplitude voltages of the primary (high-voltage, DC-bus side) and secondary (low-voltage, FC side) windings of the isolation transformer, respectively.

To compensate the short-term peak power demands of the DC-bus during the FC operation mode the power from an additional energy storage device may be required. A battery might be used in this case. Generally, to apply a battery an additional charging circuit is required, leading to increased complexity of the converter. However, by utilizing the property of the qZSI, the battery could be connected without any additional circuits, as shown in Fig. 1. The average voltage across the battery terminals equals the average capacitor *C4* voltage:

(5) $$U_B = U_{C4} = \frac{D_S}{1 - 2 \cdot D_S} \cdot U_{FC}.$$

Hence, the state-of-charge (SOC) of the battery is controlled by varying the shoot-through duty cycle D_S of the qZSI switches. The battery current depends on the voltages U_{C4} and U_B as well as on its internal resistance r_B (Fig. 5):

(6) $$i_B = \frac{U_B - U_{C4}}{r_B},$$

where U_B is the voltage rating of the battery. Hence, the state of charge of the battery depends on the voltage:

(7) $$U_{SOC} = U_B - U_{C4}.$$

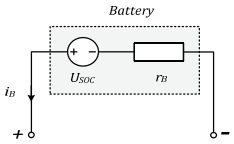

Fig. 5. Simplified equivalent circuit of a battery

In order to keep the system in continuous conduction mode (CCM) the current of the diode *D7* should never reach zero during the non-shoot-through state and the following expression should be satisfied:

(8) $$i_B < i_{Tr,2},$$

where $i_{Tr,2}$ is the current of the transformer secondary winding.

Next, the power equations for particular submodes of the FC operation mode are justified:

1. Battery assisted mode: $P_{FC} < P_{DC-bus}$

The FC and the battery provide the power to the DC-bus; the power equation is

(9) $$P_{FC} - P_{DC-bus} + P_B = 0,$$

where P_{FC} is the power of the fuel cell, P_{DC-BUS} is the power flowing into the DC-bus and P_B is the power provided by the battery. In this case $i_{L1} > i_{L2}$

2. Battery charging mode: $P_{FC} > P_{DC-bus}$

The FC supplies both the battery and the DC-bus in this case $i_{L1} > i_{L2}$ and the power equation is

(10) $$P_{FC} - P_{DC-bus} - P_B = 0.$$

3. Battery stand-by mode: $P_{FC} = P_{DC-bus}$

The fuel cell provides full power to the DC-bus and the battery is fully charged. In this case $i_{L1} = i_{L2}$ and the power equation is

(11) $$P_{FC} - P_{DC-bus} = 0.$$

Experimental verification

To validate the proposed topology the experimental setup with the power rating of 1.2 kW was assembled (Fig. 6). Operating parameters and component values of the experimental setup are listed in Table I.

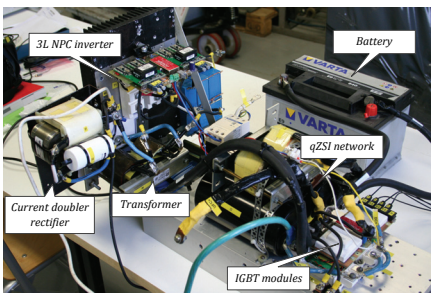

Fig. 6. Experimental 1.2 kW setup of the proposed multiport converter

Table 1. Desired operating parameters of the experimental converter

Parameter	Value
General	
DC-link voltage of the main system, $U_{DC\text{-}BUS}$	560 V
Rated voltage of the electrolyzer, U_{EL}	80 V
Light-load FC voltage, $U_{FC,max}$	70 V
Full-load FC voltage, $U_{FC,min}$	46 V
Operating frequency of the isolation transformer, f	15 kHz
Number of turns of the voltage matching transformer, $N_{Tr,1}/N_{Tr,2}/N_{Tr,3}$	24 / 6 / 15
Capacitance of C1 and C2	60 uF
Capacitance of C3 and C4	180 uF
Inductance of L1 and L2	65 uH
Inductance of L3 and L4	1.2 mH
EL mode	
Duty cycle of VSI switches, D	0.45
FC mode	
Desired voltage amplitude of the intermediate DC-link, U_1	70 V
Duty cycle of active states, D_A	0.4
Duty cycle variation of shoot-through states, D_S	0...0.17
Battery (VARTA E9)	70 Ah/12 V

A. EL operation mode

First, the system was studied in the electrolyzer mode. During the experiment no control of the output voltage was performed and 3L-NPC VSI operated with the constant duty cycle. The experimental voltage and current waveforms of the RES- and EL-side ports are presented in Fig 7. The 3L-NPC half-bridge inverter had the zero-voltage switching of all transistors without any additional components (Figs. 8 and 9).

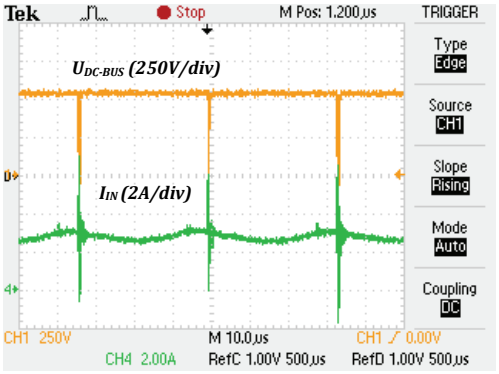

(a)

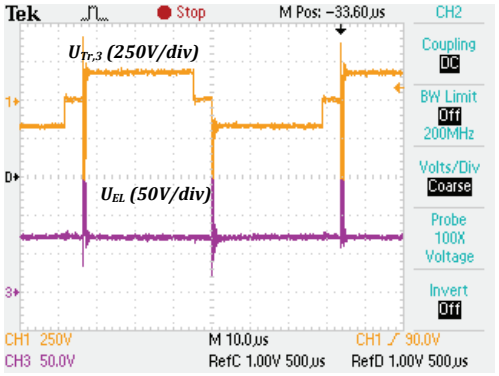

(b)

Fig. 7. Experimental waveforms of the proposed converter in the EL mode: input voltage and current of the RES-side port (a) and output voltage of the EL-side port (b)

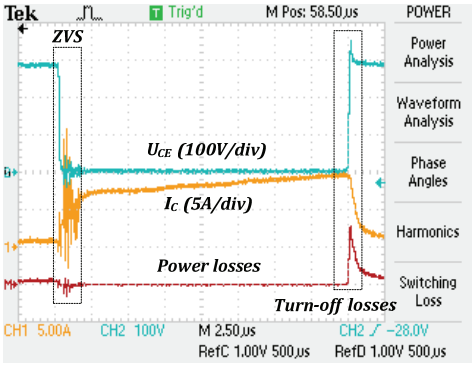

Fig. 8. ZVS operation of outer transistors (T1 and T4) of the proposed converter in the EL mode (duty cycle D=0.4)

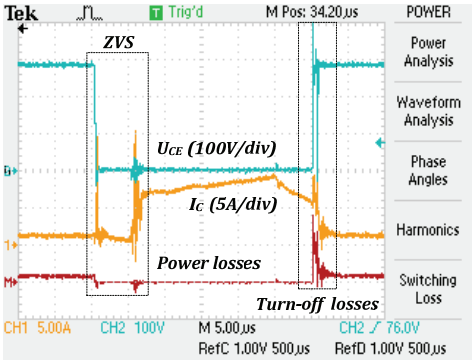

Fig. 9. ZVS operation of inner transistors (T2 and T3) of the proposed converter in the EL mode (duty cycle D=0.4)

It was found that a sufficient condition for the ZVS is that the isolation transformer should have relatively high leakage inductance of windings and the dead time implemented should be smaller than the time needed to utilize the leakage energy. Finally, it was found that by help of the proposed configuration the total losses in semiconductors in the RES-side port could be decreased by at least 25% in comparison with the topology presented in [5].

B. FC operation mode

During the fuel cell mode the converter was tested with the minimal FC voltage, thus having terminal voltage of 46 V. To boost the FC voltage to the desired voltage level of the intermediate DC-link (70 V) the shoot-through duty cycle DS was set to 0.175. In active states the isolation transformer was supplied with voltage pulses with a duty cycle of 0.35. As is seen from Fig. 10, the qZSI ensures the demanded gain of the FC voltage ($U_{FC,min} = 46$ V and $U_1 = 70$ V, as expected).

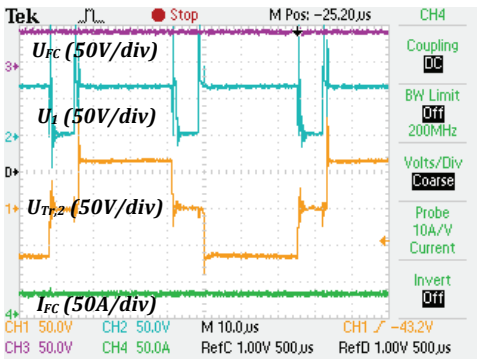

Fig. 10. Experimental waveforms of the proposed converter in the FC mode at the minimal FC voltage: intermediate DC-link voltage, voltage of the secondary winding of the voltage matching transformer and fuel cell current

Further, different possibilities of the FC operation mode were tested. It was assumed that the available FC power cannot meet the increase in the load. The system without the battery (Fig. 11a) had an appreciable voltage drop at the DC-bus, while the system with the battery was able to correspond to the increased load current and provided considerably more stable output voltage (Fig. 11b).

Assuming an initial output power P of 1 kW, the transformer current during this test can be calculated by

$$i_{Tr,2} = \frac{P \cdot (1 - 2 \cdot D_S)}{U_{FC}} = 14.1(A) \cdot \quad (12)$$

Hence, the battery current should not exceed this value in order to keep the system in CCM. Using Eq. (5) we can obtain the initial voltage across the battery (U_{C4}=12.4 V). Since the battery was fully charged, its initial current was close to zero.

After the load change to 1.2 kW, the battery current increased to 10 A. Having the battery internal resistance of 40 mΩ, we obtain:

$$U_{C4} = U_B - (i_B \cdot r_B) = 11.6(V). \quad (13)$$

Assuming the intermediate DC-link voltage variation due to the battery within 1 V, the output voltage variation is

$$\Delta U_{DC-BUS} = 2 \cdot \Delta U_{DC-link} \cdot \frac{N_{Tr,1}}{N_{Tr,2}} = 8(V), \quad (14)$$

which is acceptable within the required range of 5%.

The 3L-NPC half-bridge topology operating in the rectifier mode provided the demanded voltage doubling effect of the peak voltage of the secondary winding of the isolation transformer, thus ensuring the ripple-free voltage of 560 V DC at the DC-bus of a RES (Fig. 11b), while the maximal voltage across IGBT modules was approximately one-half of the output voltage (Fig. 12).

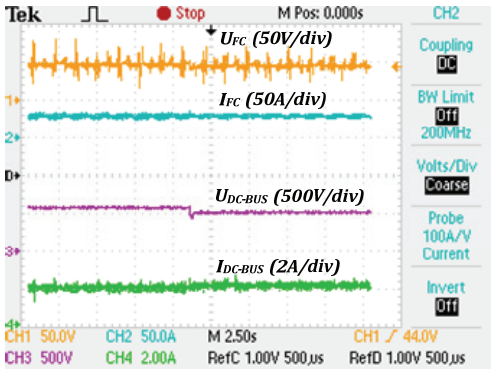

(a)

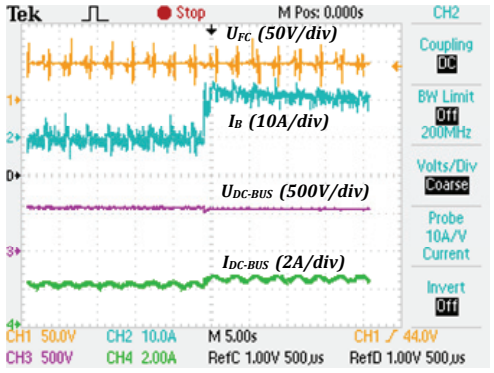

(b)

Fig. 11. Experimental waveforms of the proposed converter in the FC mode at the minimal FC voltage and limited current when the load increases: without the battery (a); with the battery (b)

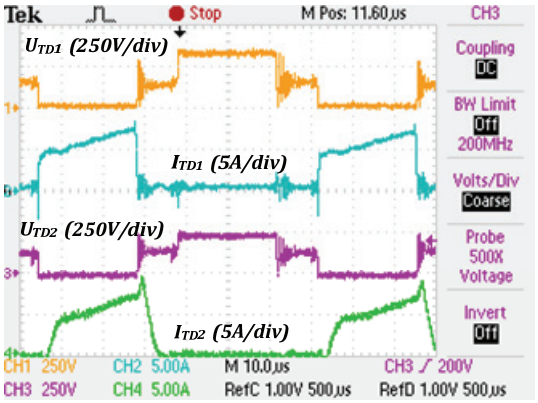

Fig. 12. Experimental waveforms of the proposed converter in the FC operating mode at the minimal FC voltage: freewheeling diode *TD1* and *TD2* voltage and current

Fig. 13 shows the battery state changing from charging to discharging during the operation with limited FC current when the load suddenly increases. As estimated, during charging $i_{L1}>i_{L2}$ and when the battery supplies the load $i_{L1}>i_{L2}$. Since the battery voltage remains relatively constant during the operation, the intermediate DC-link voltage of the qZSI is stable.

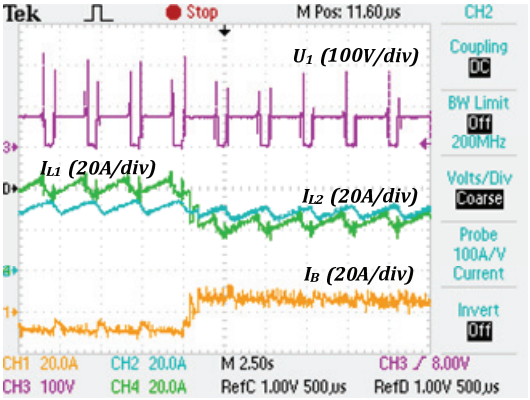

Fig. 13. Intermediate DC-link voltage, current of the inductors *L1* and *L2* and battery current during the operation with limited current when the load increases

Conclusions

The proposed novel integrated multiport DC/DC converter for hydrogen-based energy storages is capable of ensuring stabilized supply voltage for the electrolyzer as well as providing the regulated voltage on the DC-bus despite the variation of the fuel cell voltage with the load. During the hydrogen production mode (electrolyzer mode) the converter acts as a VSI-based step-down DC/DC converter while in the power back-up (fuel cell) mode the converter operates as a qZSI-based step-up DC/DC converter. The battery integrated to the FC-side port will help to balance the power difference between the FC and the load and finally improve the dynamic response of the hydrogen buffer.

In the research it was found that a 3L-NPC topology with a dedicated control algorithm in a RES-side port allows losses in the semiconductors to be reduced by at least 25%. The integration of a battery in a FC-side port require no additional charging circuit. At the same time stabilized output voltage during short-term high power demands is provided when the available FC power cannot meet the increase in the load.

Acknowledgment

This research work has been supported by Estonian Ministry of Education and Research (Project SF0140016s11), Estonian Science Foundation (Grants ETF8538) and European Social Fund (project "Doctoral School of Energy and Geotechnology II").

REFERENCES

[1] Zobaa, A.F.; Cecati, C., "A comprehensive review on distributed power generation", International Symposium on Power Electronics, Electrical Drives, Automation and Motion, SPEEDAM'2006, pp. 514-518, 23-26 May 2006.

[2] Cavallaro, C.; Chimento, F.; Musumeci, S.; Sapuppo, C.; Santonocito, C. "Electrolyser in H2 Self-Producing Systems Connected to DC Link with Dedicated Phase Shift Converter", International Conference on Clean Electrical Power, ICCEP '2007, pp. 632-638, 21-23 May 2007.

[3] del Real, A.J.; Arce, A.; Bordons, C. "Hybrid model predictive control of a two-generator power plant integrating photovoltaic panels and a fuel cell", 46th IEEE Conference on Decision and Control, pp. 5447-5452, 12-14 Dec. 2007.

[4] Ibanez, F.; Perez-Navarro, A.; Sanchez, C.; Segura, I.; Bernal, E.; Paya, J. "Wind generation stabilization using a hydrogen buffer", European Conference on Power Electronics and Applications, pp. 1-10, 2-5 Sept. 2007.

[5] Vinnikov, D.; Andrijanovits, A.; Roasto, I.; Jalakas, T.; "Experimental study of new integrated DC/DC converter for hydrogen-based energy storage," 2011 10th International Conference on Environment and Electrical Engineering (EEEIC), pp. 1-4, 8-11 May 2011

[6] Tao, H.; Kotsopoulos, A.; Duarte, J.L.; Hendrix, M.A.M. "Family of multiport bidirectional DC-DC converters", IEE Proceedings on Electric Power Applications, vol. 153, no. 3, pp. 451- 458, 1 May 2006.

[7] Tao, H.; Duarte, J.L.; Hendrix, M.A.M. "Multiport converters for hybrid power sources", IEEE Power Electronics Specialists Conference, PESC'2008, pp. 3412-3418, 15-19 June 2008.

[8] Andrijanovitš, A; Egorov, M; Lehtla, M; Vinnikov, D. "A Hydrogen Technology as Buffer for Stabilization of Wind Power Generation", 8th International Symposium "Topical Problems in the Field of Electrical and Power Engineering", Doctoral School of Energy and Geotechnology, pp. 62-70, 2010.

[9] Cavallaro, C.; Cecconi, V.; Chimento, F.; Musumeci, S.; Santonocito, C.; Sapuppo, C. "A Phase-Shift Full Bridge Converter for the Energy Management of Electrolyzer Systems", IEEE International Symposium on Industrial Electronics, ISIE'2007, pp. 2649-2654, 4-7 June 2007.

[10] Ugartemendia, J.J.; Ostolaza, X.; Moreno,V.; Molina, J.J.; Zubia; I. "Wind generation stabilization of fixed speed wind turbine farms with hydrogen buffer", 11th. Spanish-Portuguese Conference on Electrical Engineering (11CHLIE), pp. 1-5, 1-4 July 2009.

[11] Andrijanovitš, A.; Egorov, M.; Lehtla, M.; Vinnikov, D. "New Method for Stabilization of Wind Power Generation Using an Energy Storage Technology". Journal on Agronomy Research, vol. 8, (S1), pp. 12-24, May 2010.

[12] Andrijanovits, A.; Vinnikov, D.; Roasto, I.; Blinov, A.; , "Three-level half-bridge ZVS DC/DC converter for electrolyzer integration with renewable energy systems," 2011 10th International Conference on Environment and Electrical Engineering (EEEIC), pp. 1-4, 8-11 May 2011.

[13] Cintron-Rivera, J.G.; Yuan Li; Shuai Jiang; Peng, F.Z.; "Quasi-Z-Source inverter with energy storage for Photovoltaic power generation systems," 2011 Twenty-Sixth Annual IEEE Applied Power Electronics Conference and Exposition (APEC), pp.401-406, 6-11 March 2011.

[14] Vinnikov, D.; Roasto, I. "Quasi-Z-Source-Based Isolated DC/DC Converters for Distributed Power Generation", IEEE Transactions on Industrial Electronics, vol. 58, no.1, pp. 192-201, Jan. 2011.

[15] Martins, J. F.; Joyce, A.; Rangel, C.; Sotomayor, J.; Castro, R.; Pires, A.; Carvalheiro, J.; Silva, R. A.; Viana, S.; "RenH2 – Stand-Alone Energy System Supported by Totally Renewable Hydrogen Production"; Proc. of POWERENG 2007, April 12-14, 2007, Setúbal, Portugal.

***Authors**: M.Sc. Anna Andrijanovits, Tallinn University of Technology, Dep. of Electrical Drives and Power Electronics, Ehitajate tee 5, 19086 Tallinn, Estonia, E-mail: anna.andrijanovits@ieee.org; M. Sc. Andrei Blinov, Tallinn University of Technology, Dep. of Electrical Drives and Power Electronics, Ehitajate tee 5, 19086 Tallinn, Estonia, E-mail: andrei.blinov@ieee.org; Dr. Dmitri Vinnikov, Tallinn University of Technology, Dep. of Electrical Drives and Power Electronics, Ehitajate tee 5, 19086 Tallinn, Estonia, E-mail: dmitri.vinnikov@ieee.org; Dr. João Martins, Universidade Nova de Lisboa-FCT-DEE and UNINOVA-CTS, P-2829-516 Monte de Caparica, Portugal, E-mail: jf.martins@fct.unl.pt*